circularly but not linearly polarized light, the contributions to the noise spectrum due to the spontaneous and induced effects are now different: the contribution of the induced effect remains unchanged (apart from a constant factor), whereas the Zeeman line disappears from the spontaneous radiation. This can be used to distinguish the effects in doubtful cases.

The authors are grateful to V. I. Perel' for a valuable discussion.

[1]E. V. Aleksandrov, O. V. Konstantinov, V. N. Kulyasov, A. B. Mamyrin, and V. I. Perel', Zh. Eksp. Teor. Fiz. 61, 2259 (1971) [Sov. Phys. JETP 34, 1210 (1972)].
[2]R. Glauber, in: Kvantovaya optika i kvantovaya radiofizika, (Quantum Optics and Quantum Radiophysics), Russ. Transl., ed. by O. V. Bogdankevich and O. N. Krokhin, Mir, M., 1966.
[3]D. F. Smirnov, I. V. Sokolov, and A. S. Troshin, Vestn. Leningr. Univ. Fiz. Khim, No. 2, 36 (1977).
[4]O. V. Konstantinov and V. I. Perel', Zh. Eksp. Teor. Fiz. 39, 197 (1960) [Sov. Phys. JETP 12, 142 (1961)].
[5]Yu. M. Golubev and L. I. Plimak, Opt. Spektrosk. 48, 222 (1980) [Opt. Spectrosc. (USSR) 48, 126, (1980)].
[6]D. A. Varshalovich, A. N. Moskalev, and V. K. Khersonskiĭ, Kvantovaya teoriya uglovogo momenta (Quantum Theory of Angular Momentum), Nauka, L., 1975.

Translated by A. Tybulewicz

Effect of pressure on the parameters of the energy spectrum of graphite

N. B. Brandt, A. S. Kotosonov, S. V. Kuvshinnikov, and M. V. Semenov

Moscow State University
(Submitted 6 February 1980)
Zh. Eksp. Teor. Fiz. 79, 937–946 (September 1980)

The dependence of the extremal sections and of the effective masses of the carriers of pyrolytic graphite were investigated at pressures up to 17 kbar and temperatures 2–4 K. A nonlinear variation of the extremal sections S of the Fermi surface was observed at high pressures, and it is shown that this variation becomes linear when plotted in the coordinates S and V, where S is the specimen volume. The logarithmic derivatives of the extremal sections of the Fermi surface and of the effective masses of the electrons and holes with respect to pressure are determined. The logarithmic derivatives with respect to pressure are calculated for the parameters of the electron energy spectrum of graphite, and a comparison is made with the results of other experimental and theoretical studies.

PACS numbers: 71.25.Hc, 71.25.Jd

INTRODUCTION

Graphite and synthetic carbon materials on its base have a number of unique properties and have recently found extensive practical use. The distinct layered crystal structure of graphite causes all its properties to be highly anisotropic, since the interaction of the carbon atoms within each layer exceeds by one order of magnitude and interaction between atoms in neighboring layers.

A universally accepted model of the energy spectrum of graphite is at present the Slonczewski–Weiss model,[1] in which the interaction between layers is taken into account by perturbation theory. The semimetallic properties are due to the presence of a weak interaction between atoms of different layers, an interaction described by the parameters γ_i $(i=1-6)$,[1] which are small compared with the parameter γ_0 that corresponds to the interaction of the atoms in the layer. The Fermi surface of graphite consists of electron and hole parts that are strongly elongated along the $H-K-H$ edge of the Brillouin zone.

In the Slonczewski–Weiss model, the effective masses m^* and the extremal sections of the Fermi surface in the basal plane perpendicular to the hexagonal c axis of the crystal lattice are respectively described by the following formulas:

$$m_e^*(\Psi)=\frac{4}{3}\left(\frac{\hbar}{a_0}\right)^2\frac{\gamma_1}{\gamma_0^2}\cos\Psi\Big/\left(1+\frac{4\gamma_4}{\gamma_0}\cos\Psi\right), \tag{1}$$

$$m_h^*(\Psi)=\frac{4}{3}\left(\frac{\hbar}{a_0}\right)^2\frac{\gamma_1}{\gamma_0^2}\cos\Psi\Big/\left(1-\frac{4\gamma_4}{\gamma_0}\cos\Psi\right), \tag{2}$$

$$S_e=\frac{3\pi\hbar^2}{4\gamma_0^2a_0^2}\frac{2\gamma_2-\varepsilon_F}{(1+2\gamma_4/\gamma_0)^2}(\Delta-2\gamma_1+2\gamma_5+\varepsilon_F), \tag{3}$$

$$S_h=\frac{3\pi\hbar^2}{4\gamma_0^2a_0^2}\frac{2\gamma_2\cos^2\Psi_0-\varepsilon_F}{(1-2\gamma_4\cos\Psi_0/\gamma_0)^2}(\Delta+2\gamma_1\cos\Psi_0+2\gamma_5\cos^2\Psi_0-\varepsilon_F), \tag{4}$$

$$S_m=\frac{3\pi\hbar^2}{4\gamma_0^2a_0^2}\varepsilon_F(\varepsilon_F-\Delta), \tag{5}$$

where $\Psi=k_zc_0/2$, k_z is the wave number reckoned from the point K of the edge of the Brillouin zone, c_0 and a_0 are the parameters of the graphite crystal lattice ($c_0=6.708$ Å, $a_0=2.462$ Å for single-crystal graphite), S_e is the maximum section of the electron part of the Fermi surface, S_h is the maximum section of the hole part, S_m is the minimum section of the hole part of the Fermi surface of graphite near the point H, ε_F is the Fermi energy, $\Delta\equiv\gamma_6$, $\cos\Psi_0\approx|\varepsilon_F/6\gamma_2|^{1/2}$.

The accuracy of the cited expressions is ~10%. The

 0038-5646/80/090476-06$02.40

values of the parameters γ_i ($i=0-6$) and ε_F (in electron volts), determined from the data of oscillation, galvanomagnetic, and optical measurements, are given in Table I. The sets of the parameters are designated by the indices introduced in the paper of Dillon, Spain, and McClure[2]: A—the simplified model of Anderson *et al.*,[3] where $\gamma_3=\gamma_4=\gamma_5=0$; B and C—the models of McClure *et al.*,[2] where the parameters γ_0 and γ_3 are fixed while the remaining parameters are chosen for a best fit to the experimental results under the assumption that the number of electrons N is equal to the number of holes P (the difference between cases of B and C is due to the fact that in the experiments were observed two frequencies of de Haas–Van Alphen oscillations pertaining to small sections of the Fermi surface of graphite:

$$S_{m_1}=0.79\cdot10^{-42}\ \mathrm{G^2\cdot cm^2/sec^2},\quad S_{m_2}=0.35\cdot10^{-42}\ \mathrm{G^2\cdot cm^2/sec^2};$$

model B corresponds to the case of the larger section and model C to the smaller one); J—the model of Johnson and Dresselhaus,[4] where the parameters were obtained from optical measurements; N—the model of Nagayoshi *et al.*[5]

Considerable interest attaches to an investigation of the influence of pressure on the energy spectrum of graphite. A distinguishing feature of graphite is the large anisotropy of the compressibility[6]: $c_{33}^{-1}/c_{11}^{-1}\approx 29$ (c_{11}^{-1} is the compressibility in the basal plane, c_{33}^{-1} is perpendicular to the layers). Therefore the hydrostatic pressure on the crystal is practically uniaxial along the c axis.

Galvanometric measurements were made earlier[7,10] at high temperatures ~300–400 K on graphite specimens at pressures up to 5 kbar, and the pressure dependences of the parameters γ_1 and γ_4 were calculated. Subject to a number of simplifying assumptions, the accuracies of $\partial\ln\gamma_1/\partial p$ and $\partial\ln\gamma_4/\partial p$ are estimated by the authors at ~20 and ~100%, respectively.

Anderson *et al.*[3] and Itskevich and Fisher[11] investigated quantum oscillation effects in graphite at helium temperatures and at pressures up to 4 and 8 kbar, respectively. The extremal cross sections obtained in these studies and their logarithmic derivatives with respect to pressure are listed in Table II. The pressure dependences of the effective masses were not measured in Refs. 3 and 11, where data by others[7,10] were used to calculate the pressure dependences of the parameters of the Sonczewski-Weiss model.[1] However, the parameters of the energy spectrum of graphite depend strongly on the temperature.[2] For this reason the values of the parameters γ_1 and γ_4 and of their

TABLE I.

Parameter	Model				
	A	*B*	*C*	*J*	*N*
γ_0	2.85	3.20	3.11	3.18	2.73
γ_1	0.30	0.397	0.392	0.40	0.322
γ_2	−0.02	−0.0202	−0.0201	−0.0207	−0.0186
γ_3	0.00	0.29	0.29	0.30	0.29
γ_4	0.00	0.132	0.124	0.18	0.15
γ_5	0.00	0.0098	0.0234	−0.006	0.021
$\gamma_6=\Delta$	0.006	0.0221	−0.0049	0.005	−0.047
ε_F	−0.026	−0.0223	−0.0235	−0.0240	−0.0213

TABLE II.

Carriers	Extremal sections S, 10^{-42} g^2 cm^2 sec^2	$\partial\ln S/\partial p$, kbar^{-1}	m^*/m_0	$\partial\ln m^*/\partial p$, kbar^{-1}	References
Majority electrons (point K of Brillouin zone)	7.07	0.034±0.006			[3]
	7.03	0.039			[11]
	6.59				[16]
	6.44		0.07		[17]
	6.64				[18]
	7.03±0.14		0.058±0.002		[19]
	6.64				[20]
	6.52±0.06	0.0468±0.0009	0.058±0.003	0.017±0.003	Present work
Majority carriers (maximal section)	5.09	0.040±0.004			[3]
	4.94				[16]
	4.63		0.036		[17]
	5.15±0.12				[18]
	5.13±0.11		0.040±0.002		[19]
	4.85				[20]
	4.80±0.05	0.0485±0.0009	0.038±0.002	0.024±0.005	Present work
Minority carriers	0.79	0.06±0.015			[3]
	0.79				[21]
	0.36				[20]
	0.36±0.01		0.0038±0.0003		Present work

derivatives with respect to pressure, determined at high temperatures, can apparently not be used to calculate the pressure dependences of the remaining parameters from the data on the oscillation effects at low temperatures.

For a correct determination of the dependences of the parameters γ_i ($i=1-6$) and ε_F on the pressure it is necessary to use data obtained for the same specimen at identical temperatures. It is seen from expressions (1)–(5) that by measuring the pressure dependences of the extremal sections and of the effective carrier masses it is possible to determine the logarithmic derivatives of the parameters γ_i ($i=1-6$) and ε_F with respect to pressure (the parameter γ_0, which characterizes the interaction of the atoms in the basal plane, can be assumed in first-order approximation, in view of the low compressibility of c_{11}^{-1} of graphite, as independent of pressure). To our knowledge, these measurements were performed by us here for the first time ever. In addition, it was of interest to carry out investigations in the pressure region above 10 kbar, where x-ray diffraction data[12] indicate that the distance between the graphite layers has an essentially independent pressure dependence.

MEASUREMENT TECHNIQUE, SPECIMENS

We have investigated the quantum oscillations of the magnetic susceptibility and of the electric resistivity of samples of pyrolytic graphite at pressures up to 17.3 kbar in the temperature interval 2.1–4.2 K in fields up to 55 kOe, and also the behavior of the differential magnetic susceptibility χ at $p=1$ bar in fields up to 85 kOe.

The magnetic susceptibility was measured by a modulation technique.[13] To determine the absolute value of χ we used as references the values of the magnetic susceptibility of Bi. The measurement coils 2×1100 turns of PÉV-0.02 wire on a teflon core) were placed directly in a high-pressure chamber channel of 4.5 mm diameter. The measurements were made in a fixed-pressure chamber similar to that described by Itskevich.[14] The pressure-transmitting medium was a mix-

ture of 70% water-free kerosene and 30% transformer oil. The pressure in the chamber was determined from the shift of the superconducting transition temperature of a tin sensor placed in the immediate vicinity of the sample. The magnetic fields were produced by superconducting solenoids. We recorded simultaneously the oscillation curves at scans proportional to the direct (H) and reciprocal ($1/H$) magnetic fields. The harmonic analysis of the oscillation curves recorded in the reciprocal field were carried out with a computer by the procedure described by Moshchalkov.[15] The effective masses of the carriers m^* were determined from the temperature dependences of the oscillation amplitudes (the determination of m^* is discussed in greater detail below).

Quasi-single-crystal samples of pyrolytic graphite were obtained by deposition of carbon from the gas phase at a temperature 2100°C followed by heat treatment under pressure at ~3000°C. The quasi-single-crystals prepared in this manner had a block structure (block size in the basal plane ~0.7°). X-ray structure analysis show the individual single-crystal blocks to have a random orientation in the basal plane, and a lattice parameter $c_0 = 6730$ Å somewhat higher than that of single-crystal graphite (lattice parameter in the basal plane $a_0 = 2462$ Å). According to the data of galvanomagnetic measurements in strong magnetic field, the carrier decompensation in the investigated samples amounts to $P - N \lesssim 3 \cdot 10^{17}$ cm^{-3}, i.e., ~5% of the total carrier density.

To investigate the de Haas-van Alphen effect we used cylindrical samples ~4 mm long in the c-axis direction and of ~3 mm diameter. The samples used for the study of the galvanomagnetic effects were thin (~0.1 mm) plates with potential and Hall contacts to which copper electrodes were secured with silver paste.

The accuracy of the calibration of the magnetic field H was ~0.5%, that of the determination of the large Fermi-surface sections S was ~1%, that of the pressure p was ~0.1 kbar, of the absolute magnetic susceptibility χ was ~2% relative to the calibration, and $\partial \ln S / \partial p$ ~2%.

MEASUREMENT RESULTS

Figure 1 shows plots of the oscillating part of the differential magnetic susceptibility χ and of the magnetoresistance $\Delta\rho$ against the magnetic field $H \| c$ (except for special cases, all the result that follow pertain to this magnetic-field direction). Figure 2 shows plots of the spectral density of the de Haas–van Alphen oscillations at various pressures.

The extremal sections and the effective masses at pressure 1 bar, as well as the logarithmic derivatives of these quantities with respect to pressure (at $p < 10$ kbar) obtained by us and by others, are listed in Table II.

The magnetic-susceptibility oscillations in fields stronger than 4 kOe constitute a superposition of two frequencies corresponding to the electron and hole parts of the Fermi surface, whereas the oscillations of

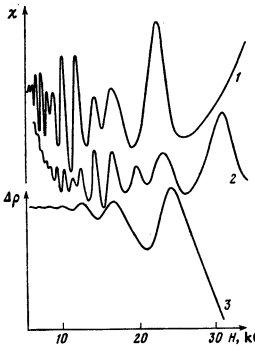

FIG. 1. Oscillations of magnetic susceptibility at pressures 4.9 kbar (1) and 17 kbar (2) and of the magnetoresistance at $p = 1$ bar in pyrographite at $T = 2.1$ K. $H \| c$.

the magnetoresistance are monochromatic (Fig. 1). The cross section determined from the Shubnikov–de Haas effect amounts to $(4.85 \pm 0.05) \times 10^{-12}$ G^{2}cm^2/sec^2 at $p = 1$ bar and pertains thus to the hole part of the Fermi surface. No oscillations of the magnetoresistance from the electron part of the Fermi surface were observed. The angular dependences of the large extremal sections of the electron and hole Fermi surface S_e and S_h, obtained by measuring the phase shift of the de Haas–van Alphen oscillations in fields up to 55 kOe, can be traced all the way to angles $\theta \sim 70°$ and are similar in character to the angular dependences obtained for natural single-crystal graphite.[20] It appears that by virtue of the high symmetry of the Fermi surface of graphite the random orientation of the single-crystal blocks in the basal plane has practically no effect on the results of these measurements.

Figure 3 shows the plots of the extremal sections S_e and S_h against pressure, determined from the de Haas–van Alphen and Shubnikov– de Haas oscillation frequencies. It is seen that at pressures p higher than 10 kbar these plots differ greatly from straight lines.

Figure 4 shows the absolute susceptibilities measured at $p = 1$ bar in fields up to 85 kOe. The arrows indicate the fields, calculated by Ono and Sugihara, corresponding to the intersections of the Fermi level with the Landau levels numbered $n = 1$–5 for the electron part and $n = 1$–3 for the hole part of the Fermi surface. As seen from this figure, in strong magnetic fields some paramagnetic maxima of the oscillations are quite well resolved, so that the effective masses m^* of the carriers can be calculated from the temperature depen-

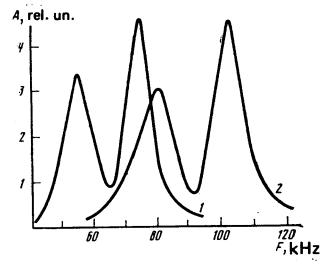

FIG. 2. Plots of the spectral density of the magnetic-susceptibility oscillations at pressures 4.9 kbar (1) and 17.3 kbar (2) (F is the oscillation frequency).

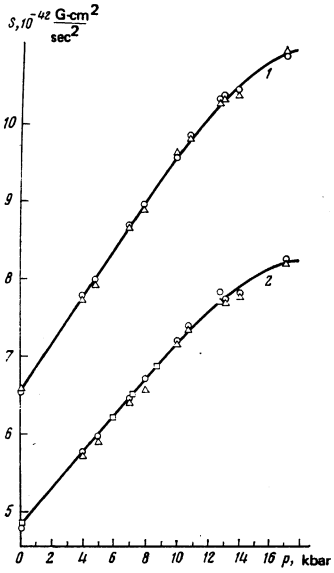

FIG. 3. Plots of the extremal sections S_e (1) and S_h (2) of pyrographite vs pressure, obtained in investigations of the de Haas–van Alphen (○—4.2 K, △—2.1 K) and of the Shubnikov–de Haas (□—4.2 K) effects; $H \parallel c$.

dences of the amplitudes of individual oscillations pertaining to the electron or hole parts of the Fermi surface. We chose for the calculation of m^* the oscillations corresponding to the Landau levels numbered $n \geq 2$, for which the position of the Fermi level differs little from its position in weak magnetic fields. We note that the effective masses of pyrographite cannot be determined from the plots of the spectral densities of the oscillations at various temperature by the method proposed by Moshchalkov,[15] since the approximations used by him are inapplicable in the present case.

The Dingle temperature T_D was determined from the Shubnikov–de Haas effect, which amounts to (6.8± 0.2) K at $p=1$ bar and increases with increasing pressure at a rate (0.18± 0.04) K/kbar. The values of T_D are independent of temperature, within the limits of the measurement accuracy, in the 2–4 K region, so that it is correct to determine the effective masses from the temperature dependences of the oscillation amplitudes.

The values $\partial \ln H_n^e(p)/\partial p = 0.0464$ kbar^{-1} and $\partial \ln H_n^h(p)/\partial p = 0.0484$ kbar^{-1} determined from the dependences of

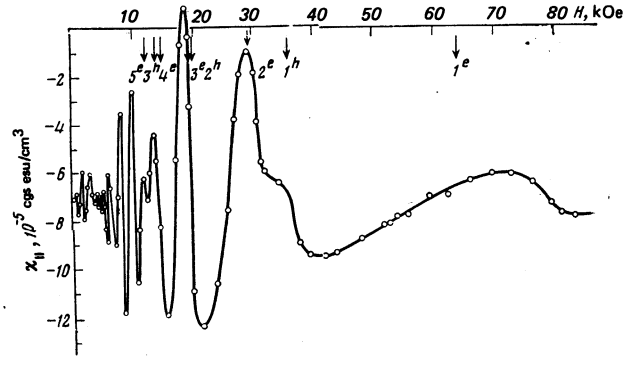

FIG. 4. Bulk differential susceptibility $\chi_{\parallel}$ of pyrographite vs magnetic field $H \parallel c$ at $p=1$ bar and $T=4.2$ K.

the relative shift of the electron and hole maxima of the de Haas–van Alphen oscillations as functions of pressures at $p < 10$ kbar [$H_n(p)$ is the field in which the corresponding oscillation maximum is observed at the pressure p] agree within the limits of error with $\partial \ln S_e/\partial p$ and $\partial \ln S_h/\partial p$ obtained from Fig. 3 (see Table II). This confirms that the oscillation maxima have been correctly assigned to the electron and hole parts of the Fermi surface.

Figure 5 shows the pressure dependences, calculated by the procedure described above from the temperature dependences of the de Haas–van Alphen oscillations, of the effective masses of the majority electrons (m_e^*) and of the majority holes (m_h^*), as well as a plot of m_h^* against pressure, obtained from an investigation of the Shubnikov–de Haas effect, where oscillations from only the majority holes were observed. It is seen that within the limits of errors (~5%) the $m_h^*(p)$ plots obtained by both methods agree. The smaller scatter of the points on the $m_e^*(p)$ plot compared with $m_h^*(p)$ is due to the better resolution of the oscillation maxima from the Landau levels of the electrons.

The extremal sections and the effective masses of the carriers were determined both with increasing and decreasing pressures in the chamber; their variation was reversible within the limits of errors, and the cross sections and masses returned to their initial values after the removal of the pressure.

Since there is no meeting of minds in the literature concerning the sizes of the small sections of the Fermi surface of graphite and concerning the positions of these groups of carriers in the Brillouin zones, we investigated the oscillations of the magnetic susceptibility in weak fields at $p=1$ bar and their angular dependence (see Fig. 6 and Table II). As seen from Fig. 6(b), the observed cross section increases with increasing angle θ between the directions of the magnetic field and of the c axis more rapidly than $1/\cos\theta$. This seems to indicate that the section S_m belongs to the neck of the hole part of the Fermi surface near the point H of the Brillouin zone.

The obtained values of the sections S_e and S_h of the investigated samples at $p=1$ bar are somewhat lower than those of single-crystal graphite (see Table II), and the absolute value of the susceptibility in weak fields, $|\chi|_{H\to 0} \approx 7.0 \cdot 10^{-5}$ cgs esu/cm^3 is somewhat high-

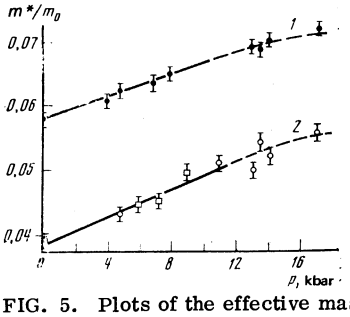

FIG. 5. Plots of the effective masses m^* of the majority electrons (1) and holes (2) vs pressure p for pyrographite (●, ○—de Haas–van Alphen effect, □—Shubnikov–de Haas effect); $H \parallel c$.

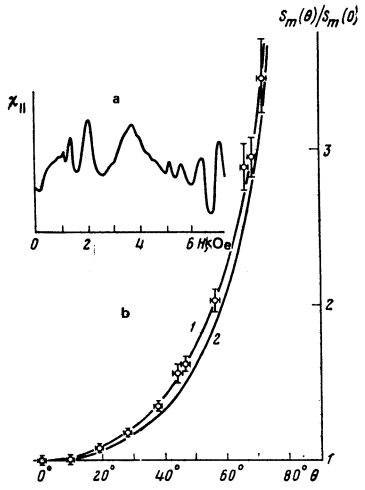

FIG. 6. Oscillations of the magnetic susceptibility in pyrographite in weak fields at H ∥ c and $p=1$ bar (a), and plot of the ratio $S_m(\theta)/S_m(0)$ for the small extermal section vs the angle θ between the directions of the magnetic field and the c axis (curve 1); curve 2 is a plot of $1/\cos\theta$.

er (according to the data of Refs. 17 and 23, $|\chi|_{H\to 0} \approx 6.8\cdot 10^{-5}$ cgs esu/cm^3 for single crystal graphite). This is apparently due to the higher value of the lattice parameter c_0 of the investigated pyrographite samples.

We note that beyond the ultraquantum limit ($H \gtrsim 72$ kOe) the susceptibility remains diamagnetic and does not differ in order of magnitude from $\chi|_{H\to 0}$ (see Fig. 4). This result agrees with the data of Chouteau and Briggs,[24] who investigated the field dependence of the magnetization of pyrographite up to 150 kOe, but disagrees with the data of Wallace and Gupta,[25] who took no account of the contribution of the filled bands to the susceptibility.

DISCUSSION OF RESULTS

To calculate the logarithmic derivatives of the parameters γ_i ($i=1-6$) and ε_F with respect to pressure it is necessary to use, in addition to the pressure dependences of the four characteristics of the electron energy spectrum of pyrographite (two extremal sections of the Fermi surface and two carrier effective masses) a number of additional assumption based on considerations of the symmetry of the graphite crystal lattice.

Dillon, Spain, and McClure[2] have considered three possible approximations for the connection between the logarithmic derivatives of the parameters γ_i ($i=1-6$) with respect to pressure. These approximation are based on the fact that small parameters γ_i ($i=1-6$) are the result of the overlap of wave functions that decrease exponentially at large distances.[8] In approximation I

$$\frac{\partial \ln|\gamma_2|}{\partial p}=\frac{\partial \ln|\gamma_5|}{\partial p}=2\frac{\partial \ln\gamma_1}{\partial p}, \tag{6}$$

$$\frac{\partial \ln\gamma_3}{\partial p}=\frac{\partial \ln\gamma_4}{\partial p}; \tag{7}$$

in approximation II

$$\frac{\partial \ln|\gamma_2|}{\partial p}=\frac{\partial \ln|\gamma_5|}{\partial p}, \tag{8}$$

TABLE III.

	S_e	S_h	S_m	m^*_e/m_0	m^*_h/m_0	m^*_m/m_0
Calculation[2]	7.09	5.04	0.35	0.059	0.043	0.004
Experiment (present work)	6.92	5.14	0.36 [1)]	0.059	0.040	0.0038 [1)]

[1)]The values are given for $p=1$ bar; the values of S_m and m^*_m in the pressure region up to 1.2 kbar remain constant within the limits of the measurement accuracy. No reliable data could be obtained concerning the variation of these values at high pressures could be obtained.

$$\frac{\partial \ln\gamma_1}{\partial p}=\frac{\partial \ln\gamma_3}{\partial p}=\frac{\partial \ln\gamma_4}{\partial p}, \tag{9}$$

and in approximation III

$$\frac{\partial \ln|\gamma_2|}{\partial p}=\frac{\partial \ln|\gamma_5|}{\partial p}=2\frac{\partial \ln\gamma_1}{\partial p}$$
$$=2\frac{\partial \ln\gamma_3}{\partial p}=2\frac{\partial \ln\gamma_4}{\partial p}. \tag{10}$$

From Eqs. (1) and (2) and from the $m^*_e(p)$ and $m^*_h(p)$ dependences obtained in the present paper it follows that $\partial \ln\gamma_1/\partial p \neq \partial \ln\gamma_4/\partial p$, which does not agree with approximations II and III. We have therefore used approximation I in the calculations.

The minimum section S_m determined experimentally in the present study agrees well with the calculated one for the set of parameters C of the graphite spectrum (see Table I); the parameter sets A, B, J, and N yield approximately double the value of S_m.[2]

The set of parameters C describes well the values of the extremal sections and of the effective masses of single-crystal graphite. In the investigated pyrographite samples, the distance between layers is ~0.3% larger, but under pressure it decreases and at a certain pressure p_0 it becomes close to the interlayer distance of single-crystal graphite. The variation of the interlayer distance in graphite at pressures up to 16 kbar was investigated by Kabalkina and Vershchagin[12] and is described by the following empirical formula:

$$\Delta c_0(p)/c_0(0) = -28\cdot 10^{-7}p + 45\cdot 10^{-12}p^2, \tag{11}$$

where p is the pressure in bars, $c_0(0)$ is the lattice parameter at $p=1$ bar, $c_0(p)$ is the value of this constant at the pressure p, and $\Delta c_0(p) = c_0(p) - c_0(0)$. The value of p_0 obtained for our samples from (11) is ~1.2 kbar.

Table III lists the extremal sections and effective masses calculated at $p=1$ for the set of parameters C, and our data recalculated for a pressure $p_0=1.2$ kbar. The cross sections are given in units of 10^{-42} g^{2}cm^2/sec^2.

In Table IV are given the values of $\partial \ln\gamma_i/\partial p$ ($i=1-6$) and $\partial \ln\varepsilon_F/\partial p$ (in kbar^{-1}) calculated[2] for the set of pa-

TABLE IV.

	$\frac{\partial \ln\gamma_1}{\partial p}$	$\frac{\partial \ln\gamma_2}{\partial p}$	$\frac{\partial \ln\gamma_3}{\partial p}$	$\frac{\partial \ln\gamma_4}{\partial p}$	$\frac{\partial \ln\gamma_5}{\partial p}$	$\frac{\partial \ln\gamma_6}{\partial p}$	$\frac{\partial \ln\varepsilon_F}{\partial p}$
Calculation[2]	0.021	0.042	0.075	0.075	0.042	−0.036	0.022
Experiment (present work)	0.022	0.043	0.032	0.032	0.043	−0.048	0.023

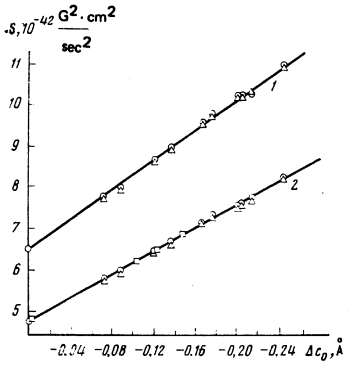

FIG. 7. Extremal sections S_e (1) and S_h (2) at $H \| c$ vs change $\Delta c_0(p)$ of the lattice parameter of pyrographite.

rameters C in approximation I [Eqs. (6) and (7)] and the corresponding experimental values for $p < 10$ obtained by us here from Eqs. (1)–(5) in approximation I for the same set of parameter. To calculate the experimental values of the logarithmic derivatives of the spectrum parameters, we used the quantities

$$\partial \ln S_e/\partial p, \quad \partial \ln S_h/\partial p, \quad \partial \ln m_e^*/\partial p, \quad \partial \ln m_h^*/\partial p,$$

recalculated for the pressure p_0 [thus, $\partial \ln S/\partial p = (S(p) - S(p))/(p - p_0)S(p_0)$].

The accuracy of the values $\partial \ln\gamma_i/\partial p$ $(i = 1-6)$ and $\partial \ln\varepsilon_F/\partial p$ obtained here is ~20% and is limited mainly by the error in the determination of the effective carrier masses and by the accuracy of the initial equations (1)–(5). As seen from Tables III and IV, our results agree sufficiently well with the calculated data,[2] obtained within the framework of the Slonczewski-Weiss model.

The deviation of the plots of S_e and S_h vs. p from straight lines in the pressure region above 10 kbar, which to our knowledge was observed here for the first time ever, is apparently due connected with the circumstance that the interlayer distance in graphite has a nonlinear pressure dependence.[12] Figure 7 shows plots of S_e and S_h against the change $\Delta c_0(p)$ of the lattice parameter calculated from Eq. (11). It is seen from the figure that these plots are close to linear in a wide range of variation of the interlayer distance (up to ~3.5%). Owing to the low compressibility c_{11}^{-1}, this means that the sections of the Fermi surface depend linearly also on the volume V of the sample.

[1]J. C. Slonczewski and P. R. Weiss, Phys. Rev. **109**, 272 (1958).
[2]R. O. Dillon, I. L. Spain, and J. W. McClure, J. Phys. Chem. Sol. **38**, 635 (1977).
[3]R. J. Anderson, W. J. O'Sullivan, J. E. Shirber, and D. E. Soule, Phys. Rev. **164**, 1038 (1967).
[4]L. G. Johnson and G. Dresselhaus, Phys. Rev. **B7**, 2275 (1973).
[5]H. Nagayoshi, K. Nakao, and L. Uemura, Solid State Comm. **18**, 225 (1976).
[6]R. Nicolow, W. Wakabayashi, and H. G. Smith, Phys. Rev. **B5**, 4951 (1972).
[7]V. V. Kechin, A. I. Likhter and G. N. Stepanov, Fiz. Tverd. Tela (Leningrad) **10**, 1242 (1968) [Sov. Phys. Solid State **12**, 987 (1968)]
[8]R. G. Arkhipov, V. V. Kechin, A. I. Likhter, and Yu. A. Pospelov, Zh. Eksp. Teor. Fiz. **44**, 1964 (1963) [Sov. Phys. JETP **44**, 1321 (1963)].
[9]A. I. Likhter and V. V. Kechin, Fiz. Tverd. Tela (Leningrad) **5**, 3066 (1963) [Sov. Phys. Solid State **5**, 2246 (1964)].
[10]V. V. Kechin, Fiz. Tverd. Tela (Leningrad) **11**, 788 (1969) [Sov. Phys. Solid State **11**, 638 (1969)].
[11]E. S. Itskevich and L. M. Fisher, Pis'ma Zh. Eksp. Teor. Fiz. **5**, 141 (1967) [JETP Lett. **5**, 114 (1967)].
[12]S. S. Kabalkina and A. F. Vereshchagin, Dokl. Akad. Nauk SSSR **131**, 300 (1960) [Sov. Phys. Dokl. **5**, 373 (1960)].
[13]M. V. Semenov, Izmer, Tekhn. No. **5**, 59 (1975).
[14]E. S. Itskevich, Prib. Tekh. Eksp. No. 4, 148 (1963).
[15]V. V. Moshchalkov, Izv. vyssh. ucheb. zaved., Fizika No. 1, 58 (1978).
[16]T. G. Berlincourt and M. C. Steel, Phys. Rev. **B3**, 148 (1955).
[17]D. Schoenberg, Trans. Roy. Soc. (London) **245**, 1 (1952).
[18]J. A. Woolam, Phys. Rev. **B3**, 148 (1971).
[19]D. E. Soule, J. W. McClure, and L. B. Smith, Phys. Rev. **134**, A453 (1963).
[20]D. E. Soule, IBM J. Res. Develop. **8**, 268 (1964).
[21]S. J. Williamson, S. Foner, and M. S. Dressehaus, Phys. Rev. **140**, A1429 (1965).
[22]S. Ono and K. Sugihara, J. Phys. Soc. Japan **24**, 818 (1968).
[23]E. Poquet, N. Lumbroso, J. Hoerau, A. Marchand, A. Pacault, and D. E. Soule, J. Chim. Phys. **57**, 866 (1960).
[24]G. Chouteau and A. Briggs, Solid State Comm. **21**, 785 (1977).
[25]P. R. Wallace and O. P. Gupta, Solid State Comm. **15**, 1577 (1974).

Translated by J. G. Adashko